



**HAL**  
open science

## Application of in vitro data in physiologically-based kinetic models for quantitative in vitro-in vivo extrapolation: A case-study for baclofen

Emma E.J. Kasteel, Leonie S. Lautz, Maxime Culot, Nynke I Kramer, Anne Zwartsen

### ► To cite this version:

Emma E.J. Kasteel, Leonie S. Lautz, Maxime Culot, Nynke I Kramer, Anne Zwartsen. Application of in vitro data in physiologically-based kinetic models for quantitative in vitro-in vivo extrapolation: A case-study for baclofen. *Toxicology in Vitro*, 2021, 76, pp.105223. 10.1016/j.tiv.2021.105223 . anses-03317990

**HAL Id: anses-03317990**

**<https://anses.hal.science/anses-03317990v1>**

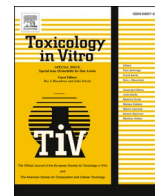
Submitted on 9 Aug 2021

**HAL** is a multi-disciplinary open access archive for the deposit and dissemination of scientific research documents, whether they are published or not. The documents may come from teaching and research institutions in France or abroad, or from public or private research centers.

L'archive ouverte pluridisciplinaire **HAL**, est destinée au dépôt et à la diffusion de documents scientifiques de niveau recherche, publiés ou non, émanant des établissements d'enseignement et de recherche français ou étrangers, des laboratoires publics ou privés.



Distributed under a Creative Commons Attribution 4.0 International License



# Application of *in vitro* data in physiologically-based kinetic models for quantitative *in vitro-in vivo* extrapolation: A case-study for baclofen

Emma E.J. Kasteel<sup>a</sup>, Leonie S. Lautz<sup>b</sup>, Maxime Culot<sup>c</sup>, Nynke I. Kramer<sup>a</sup>, Anne Zwartzen<sup>a,\*</sup>

<sup>a</sup> Institute for Risk Assessment Sciences (IRAS), Faculty of Veterinary Medicine, Utrecht University, P.O. Box 80.177, 3508TD Utrecht, the Netherlands

<sup>b</sup> Risk Assessment Department, French Agency for Food, Environmental and Occupational Health & Safety (ANSES), 14 rue Pierre et Marie Curie, Maisons-Alfort F-94701, France

<sup>c</sup> Blood-Brain Barrier Laboratory (LBHE), Faculté des Sciences Jean Perrin, Université d'Artois, Rue Jean Souvraz, F-62300 Lens, France

## ARTICLE INFO

Editor: Dr P Jennings

### Keywords:

Baclofen  
Physiologically-based pharmacokinetic modelling  
Microelectrode array (MEA)  
Quantitative *in vitro* to *in vivo* extrapolation (QIVIVE)  
Children

## ABSTRACT

Physiologically-based kinetic (PBK) models can simulate concentrations of chemicals in tissues over time without animal experiments. Nevertheless, *in vivo* data are often used to parameterise PBK models. This study aims to illustrate that a combination of kinetic and dynamic readouts from *in vitro* assays can be used to parameterise PBK models simulating neurologically-active concentrations of xenobiotics. Baclofen, an intrathecally administered drug to treat spasticity, was used as a proof-of-principle xenobiotic.

An *in vitro* blood-brain barrier (BBB) model was used to determine the BBB permeability of baclofen needed to simulate plasma and cerebrospinal concentrations. Simulated baclofen concentrations in individuals and populations of adults and children generally fall within 2-fold of measured clinical study concentrations. Further, *in vitro* micro-electrode array recordings were used to determine the effect of baclofen on neuronal activity (cell signalling). Using quantitative *in vitro-in vivo* extrapolations (QIVIVE) corresponding doses of baclofen were estimated. QIVIVE showed that up to 4600 times lower intrathecal doses than oral and intravenous doses induce comparable neurological effects. Most simulated doses were in the range of administered doses. This shows that PBK models predict concentrations in the central nervous system for various routes of administration accurately without the need for additional *in vivo* data.

## 1. Introduction

Physiologically-based kinetic (PBK) models simulate concentrations in tissues based on biokinetic properties of chemicals and physiological properties of animals and humans. These models consist of different compartments (organs and blood) to simulate time-concentration profiles of chemicals (Paini et al., 2019). Because PBK models simulate concentrations as opposed to measuring them, these models help reduce the need for expensive pre-clinical studies of pharmaceuticals and ethically questionable *in vivo* toxicity testing studies (e.g. 90-day repeat oral dose study in rat (Loizou et al., 2008; Perry et al., 2020)). Also, populations of specific interest, like children, elderly or the sick, can relatively easily be modelled, since these populations are often excluded from clinical studies. By making effective use of all available *in vitro* and *in vivo* data, PBK simulations can highlight important factors underlying kinetic variability (e.g. age, body composition, gender, (patho)physiological conditions, etc.), while minimising animal experiments (Fairman

et al., 2020; Punt et al., 2019).

In a next generation risk assessment of chemicals, the use of PBK models can provide a framework to facilitate quantitative *in vitro-in vivo* extrapolation (QIVIVE). Using QIVIVE, *in vitro* hazard characterization data can be used to predict *in vivo* therapeutic and toxic doses (Paini et al., 2019), thereby improving our mechanistic understanding of differences in therapeutic and effective doses between animals and humans. A next generation PBK (NG-PBK) model refers to a PBK model that is built, parameterised and evaluated without the need for producing new animal *in vivo* data, but instead is solely based on *in silico*, *in vitro* and/or human *in vivo* data (Paini et al., 2019).

The benefits of PBK modelling over traditional pharmacokinetic studies are especially relevant to neurologically-active chemicals due to several reasons. First, there is a paucity of adequate information on (pre-)clinical brain concentrations (Gaohua et al., 2016). Second, the brain contains various fluids, barriers and interfaces laced with transporters and ion channels with which xenobiotics (including therapeutics)

\* Corresponding author.

E-mail address: [a.zwartzen@uu.nl](mailto:a.zwartzen@uu.nl) (A. Zwartzen).

<https://doi.org/10.1016/j.tiv.2021.105223>

Received 8 December 2020; Received in revised form 21 June 2021; Accepted 14 July 2021

Available online 20 July 2021

0887-2333/© 2021 The Authors. Published by Elsevier Ltd. This is an open access article under the CC BY license (<http://creativecommons.org/licenses/by/4.0/>).

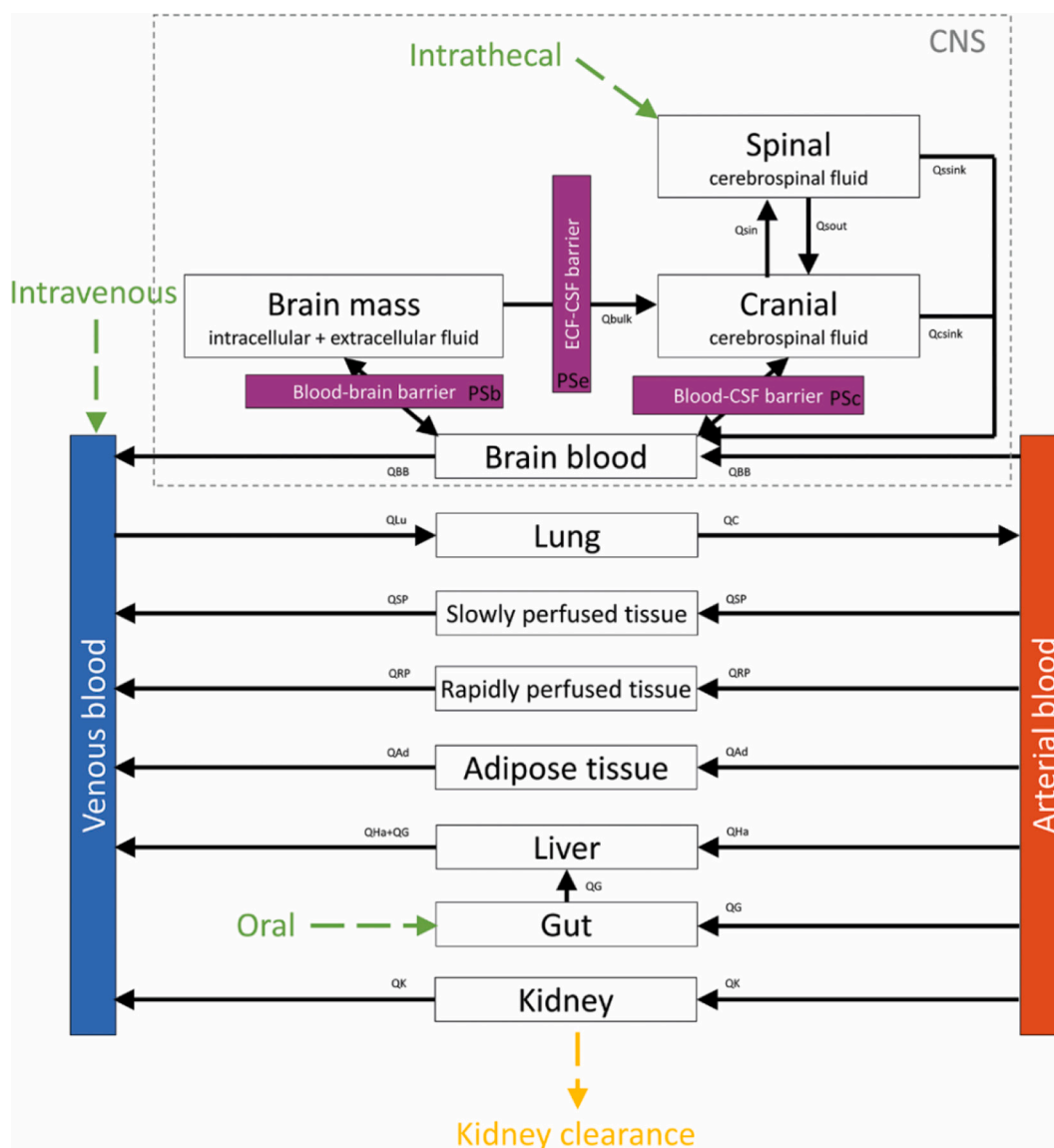


**Fig. 1.** Schematic representation of the full body PBK model with a specialised CNS compartment for baclofen. The permeability limited brain compartment is lined in grey, with the three brain barriers/interfaces depicted in purple. Administration routes (oral, intravenous, and intrathecal) are indicated in green. The route of elimination (kidney clearance) is depicted in yellow. CNS: central nervous system, CSF: cerebrospinal fluid, QK: flow to/from the kidney, QG: flow to/from the gut, QHa: hepatic artery flow, QAd: flow to/from adipose tissue, QRP: flow to/from rapidly perfused tissue, QSP: flow to/from slowly perfused tissue, QC: cardiac output, QLu: flow to the lung, QBB: flow to/from the brain, Qbulk: bulk flow from the brain mass to the cranial CSF, Qsin and Qsout: CSF shuttle flow between cranial and spinal cord CSF, Qssink and Qcsink: flow from spinal and cranial CSF compartments to blood, respectively, PSb: permeability surface area product between brain blood and brain mass, PSc: permeability surface area product between brain blood and cranial CSF, PSe: permeability surface area product between brain mass and cranial CSF.

interact (Dauer and Przedborski, 2003; Nestler et al., 2002), and cellular structures influencing the distribution of xenobiotics in the central nervous system (CNS) (de Lange, 2015; Stolp et al., 2013). Furthermore, species differences in these transporters at the blood-brainbarrier (BBB) and blood-cerebrospinal fluid (CSF) barrier (BCSFB) hamper extrapolation from animal *in vivo* data (Morris et al., 2017). Moreover, plasma concentrations are often not a satisfactory surrogate for brain concentrations due to the various barriers in the brain and the barriers surrounding the CNS (Simon et al., 2018). Therefore, subdividing the brain is important for pharmaceuticals with a CNS target site and for intrathecally administered pharmaceuticals as their distribution into the different brain regions influences target site concentrations.

The aim of this manuscript is to illustrate how effective intrathecal, oral and intravenous doses of neurologically-active xenobiotics could be predicted using NG-PBK models with a compartmentalised CNS using

solely *in silico* and *in vitro* kinetic and toxicity data as input. Since the concentrations of many neurologically-acting chemicals are influenced by active transporters and therefore plasma concentrations cannot be related to brain concentrations, in addition to validation data on total brain concentrations (CSF and brain matter) often being unavailable, the use of flow-limited models based on brain:plasma partition coefficients is not preferred. Our models build on the models of Gaohua et al. (2016); Verscheijden et al. (2019); and Yamamoto et al. (2018) using a compartmentalised CNS. Gaohua et al. (2016) developed and evaluated a brain model for paracetamol and phenytoin. Using this model as a starting point, Verscheijden et al. (2019) published a paediatric brain model that was evaluated for different analgesics, including paracetamol and ibuprofen, and the antibiotic meropenem. Moreover, Yamamoto et al. (2018) published a human PBK brain model, based on an earlier published rat PBK model, and investigated the influence of

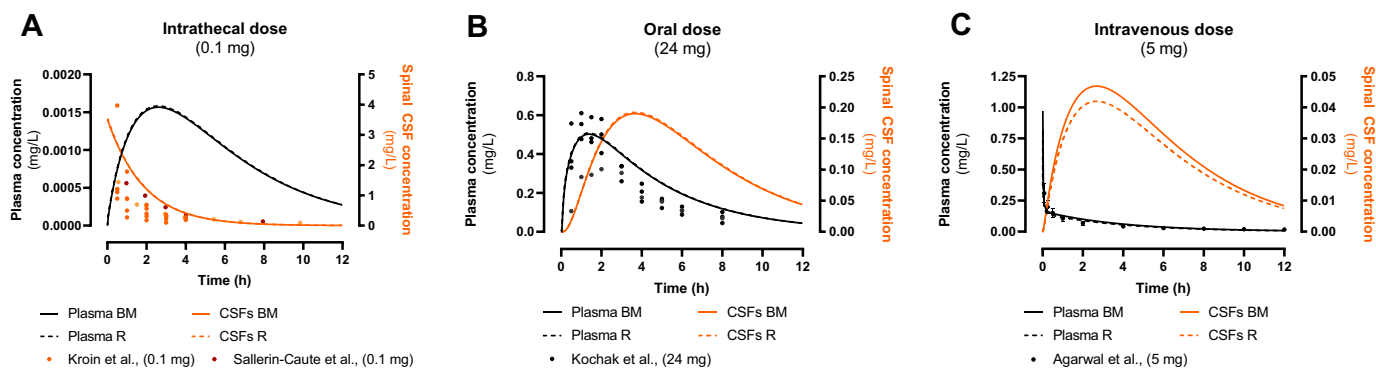


**Fig. 2.** Simulations of baclofen concentration-time profiles in a single male adult in Berkeley Madonna and R. Plasma concentrations (black lines) and spinal CSF (orange lines) are depicted following a single 0.1 mg intrathecal (A), 24 mg oral (B) or 5 mg intravenous (C) dose. Solid lines indicate simulations performed in Berkeley Madonna, whereas dashed lines indicate simulations performed in R. The dots indicate the validation data from clinical studies as described in Methods Table S4 in the Supplementary Information.

healthy and diseased CNS on concentrations of analgesics in the brain. While these models significantly improve the simulation accuracy of brain concentrations of pharmaceuticals and include a means to simulate the influence of age and pathophysiology on the pharmacokinetics of these drugs, the models are limited to simulating oral and intravenous drug administrations and have not been used for QIVIVE of neurologically-active substances. While previously published PBK models focused on various analgesics, so far no evaluated PBK model for intrathecally administered neurologically-acting chemicals is available.

Baclofen is a gamma-aminobutyric acid (GABA)-B receptor agonist often administered intrathecally to treat spasticity and also used (off-label) to treat alcohol use disorder (Simon et al., 2018). Intrathecal administration is preferred since baclofen appears to be poorly taken up across the BBB (Deguchi et al., 1995; Simon et al., 2018). Oral and intravenous doses needed to obtain CSF concentrations at therapeutic levels result in heavy side effects like drowsiness, memory impairment, ataxia and coma (Heetla et al., 2016; Meythaler et al., 2004; Sharma et al., 2018; Weißhaar et al., 2012). Since its poor permeability across the BBB, oral and intravenous doses and plasma concentrations of baclofen cannot be related to (effective) brain concentrations (Simon et al., 2018).

We describe and evaluate a NG-PBK model for baclofen, simulating concentrations in various fluids and tissues for populations (both sexes) of adults and children following intrathecal, oral and intravenous administration. In addition, individuals were modelled since the use of single patient models could aid in patient-centred treatment. This model simulates cerebral spinal fluid concentrations using *in vitro* BBB permeability data, eliminating the need for fitting of values to blood and tissue concentrations of xenobiotics measured in animal tests or human *in vivo* studies. The models were computed in both Berkeley Madonna

and R and the results were compared to available human *in vivo* pharmacokinetic measurements from clinical studies. In addition, doses affecting neuronal cell signalling (in mg) were calculated by correlating *in vitro* data obtained from neuronal activity measurements using micro-electrode array (MEA) recordings to corresponding CNS concentrations using QIVIVE.

## 2. Methods

### 2.1. PBK model structure and input parameters

The models of Verscheijden et al. (2019) and Gaohua et al. (2016) were used as a starting point to develop the CNS compartment of the baclofen PBK models for adults (age 18–50) and children (age 10). Compared to the models of Verscheijden et al. (2019) and Gaohua et al. (2016), besides the addition of chemical-specific data, the following adaptations have been made: 1) the choice of compartments was altered, since not all compartments were relevant for the kinetics of baclofen, 2) an intrathecal administration route was added, 3) physiological parameters used were based on different sources (for Gaohua et al. (2016) the model code was unavailable, Verscheijden et al. (2019) included only a paediatric model). Moreover, compared to Verscheijden et al. (2019), a different package was used in R to solve the PBK model.

All models in the current study are suitable for simulating baclofen concentration-time profiles in various organs following intrathecal, oral and intravenous administration of baclofen as all dosing routes are incorporated in the models. All organs and tissues were assumed to be homogenous and were modelled as blood-flow limited, except the CNS since the transfer rates across CNS interfaces and barriers are considered rate limiting. The CNS compartment is connected to the other tissue

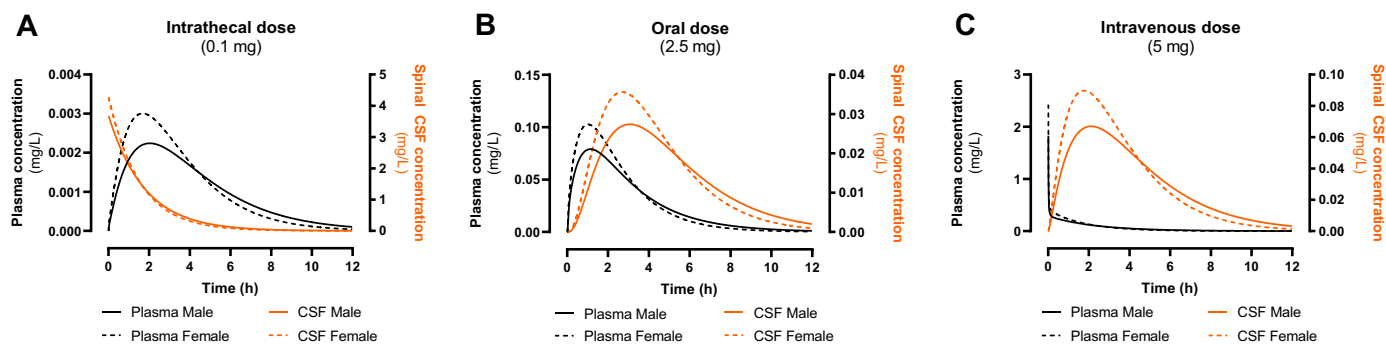


**Fig. 3.** Simulations of baclofen concentration-time profiles in a single paediatric male and single paediatric female. Plasma concentrations (black lines) and spinal CSF (orange lines) are depicted following a single 0.1 mg intrathecal (A), 2.5 mg oral (B) or 5 mg intravenous (C) dose. Solid lines indicate simulations of an adult male, whereas dashed lines indicate simulations of an adult female. Simulations were made using Berkeley Madonna.

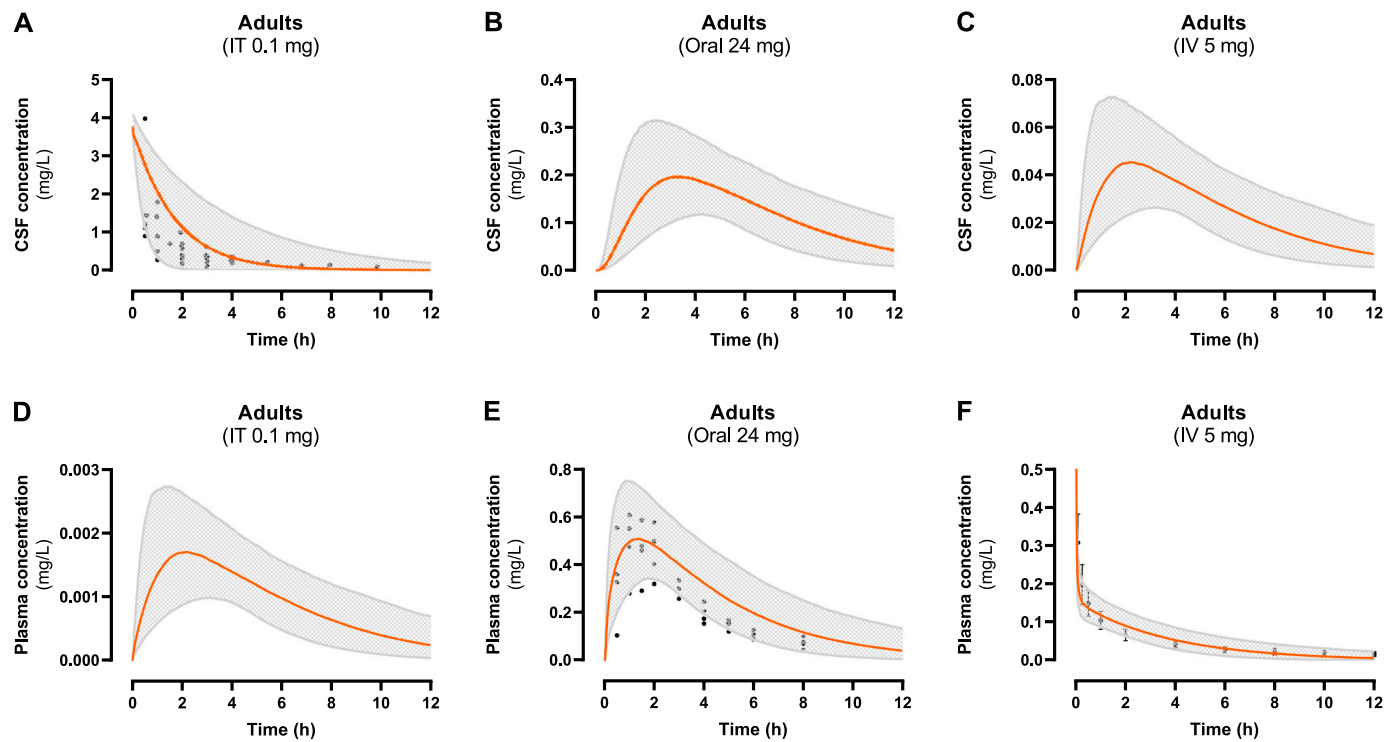


**Fig. 4.** Simulations of baclofen concentration-time profiles of an adult population. Spinal cord CSF (A–C) and plasma (D–F) concentrations are depicted following a single intrathecal dose of 0.1 mg (A, D), oral dose of 24 mg (B, E) or intravenous dose of 5 mg (C, F). The population consists of 1000 males and 1000 females. Orange lines indicate the median, while grey lines indicate the limits of the 95% confidence intervals. The dots indicate the evaluation data from multiple patients from clinical studies described in Methods Table S4 in Supplementary Information. No clinical data is available for spinal cord CSF concentrations following oral and intravenous administration, and for plasma concentrations following intrathecal administration.

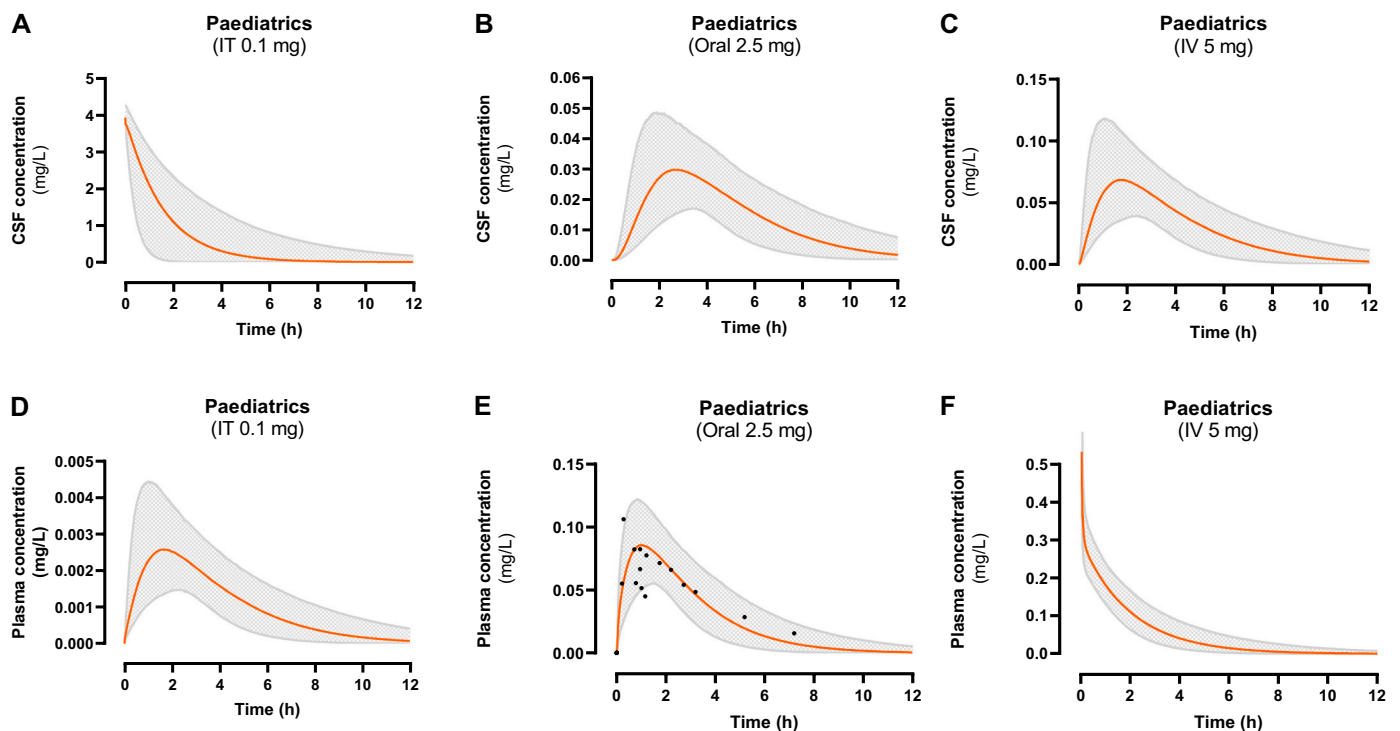


**Fig. 5.** Simulations of baclofen concentration-time profiles of a paediatric population. Spinal cord CSF (A–C) and plasma (D–F) concentrations are depicted following a single intrathecal dose of 0.1 mg (A, D), oral dose of 2.5 mg (B, E) or intravenous dose of 5 mg (C, F). The population consists of 1000 males and 1000 females. Orange lines indicate the median, while grey lines indicate the limits of the 95% confidence intervals. The dots indicate the plasma concentration evaluation data from multiple patients from a clinical study described in Methods Table S4 in Supplementary Information. For all other simulations, no evaluation data was available from literature.



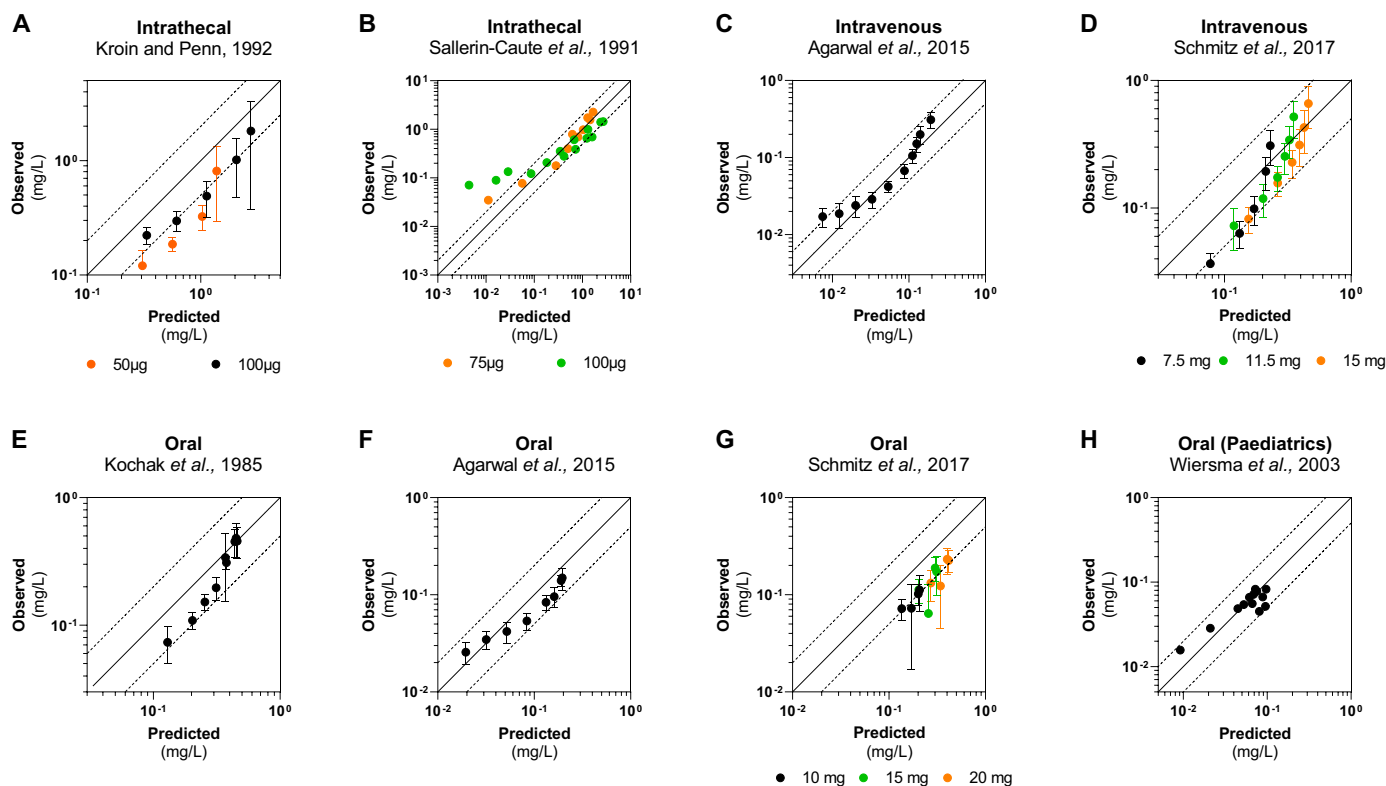


**Fig. 6.** Observed vs. predicted plots of clinical data and population-based baclofen models. Plots are shown for single intrathecal (A, B; CSF concentrations), intravenous (C, D; plasma concentrations) or oral (E, F, G; plasma concentrations) dose in adults, and single oral (H) dose in paediatric patients. The median of the simulated population was compared to the data points from the clinical data. The age, sex and body weights of the simulated populations were matched to the age, sex and body weights of the patients in the clinical study, when described in the clinical studies (for details on the patients see Methods Table S4 in Supplementary Information). The solid line indicates no deviation between observed and predicted (simulated) values. The dotted lines indicate a 2-fold deviation. For oral data, only timepoints after 30 min were considered relevant as earlier data points showed uptake not corresponding with clinically determined absorption constants.

compartments *via* the arterial and venous blood and is split into four sub-compartments: the brain mass, the brain blood, the cranial cerebrospinal fluid (CSF) and the spinal cord CSF (Fig. 1). The flows to ( $Q_{bulk}$ ), from ( $Q_{sink}$ ,  $Q_{csink}$ ) and between ( $Q_{sin}$ ,  $Q_{sout}$ ) the CSF compartments are dependent on the CSF production rate and on each other (Fig. 1; see Supplementary Models for the equations). Several assumptions are made for the CNS compartment: [1] only the free fraction of baclofen transfers across the BBB and BCSFB, [2] the barrier between brain mass and cranial CSF is completely permeable and represented by the passive permeability surface area product (PSe) (Gaohua et al., 2016), [3] there is no barrier between the cranial and spinal cord CSF, there are just fluid flows, depicted by  $Q_{sin}$  (flow from cranial to spinal cord CSF) and  $Q_{sout}$  (flow from spinal cord to cranial CSF) (Gaohua et al., 2016), [4] the barrier between the brain blood and the brain mass is the BBB (Gaohua et al., 2016) and is represented by a value for PSb (passive permeability surface area product BBB) obtained using *in vitro* experiments (see Section 2.1.1), [5] the barrier between the brain blood and the cranial CSF is the BCSFB and is represented by a value for PSc (passive permeability surface area product BCSFB), which is around two-fold smaller than corresponding BBB values, due to a  $\sim$ two-fold smaller surface area (Gaohua et al., 2016; Verscheijden et al., 2019), and [6] no metabolism of baclofen occurs in the brain.

All non-CNS compartments (*i.e.* kidney, gut, liver, adipose tissue, rapidly perfused tissue, slowly perfused tissue and lung) are included because they either influence the pharmacokinetics of baclofen by being involved in the absorption, distribution or excretion or allow for the extension of the model to simulating other xenobiotics and inhalation routes in future studies. Since baclofen is not metabolically cleared and mainly eliminated *via* urine (70–80%; Drugbank (2005)), the sole elimination route for baclofen is *via* renal clearance (clinically

determined CL<sub>urine</sub>; see Supplementary Methods Table S2).

Physiological and chemical-specific parameters were taken from literature and PK-SIM version 8, and scaled to body weight, body height, age and body surface area (see Methods Table S2 and Table S3 in Supplementary Information). Using the quantitative structure activity relationships (QSAR) described by Rodgers et al. (2005); Rodgers and Rowland (2006) for zwitterions with a strong base, partition coefficients were calculated, taking the ionization and lipophilicity of the compound into account (Rodgers et al., 2005; Rodgers and Rowland, 2006). The PBK models were scripted in Berkeley Madonna (BM) version 8.3.18 and in R version 3.6.3 using packages 'R<sub>x</sub>ODE', 'truncnorm' and 'ggplot2' (Fidler et al., 2020; Mersmann et al., 2018; R Development Core Team, 2018; Wickham, 2016). The model codes are found in the Supplementary Information ('Supplementary Models').

### 2.1.1. *In vitro* BBB permeability

Regarding its CNS distribution, baclofen has been reported to be a substrate for both influx and efflux transporters expressed at the BBB *in vivo* in rats, respectively, the large neutral amino acid transporter (LAT1, aka SLC7A5) (Simon et al., 2018) and the organic anion transporter 3 (OAT3) (Deguchi et al., 1995; Simon et al., 2018). No information is available on the transporters involved in transport of baclofen across the BBB in humans. The expression level of OAT3 in humans is  $>5$ -fold smaller than in rats, if OAT3 is present at all (Hoshi et al., 2013). This implicates that it is unlikely that OAT3 is the main efflux transporter responsible for the efflux of baclofen across the BBB in humans. The permeability of the BBB by baclofen was measured *in vitro* using a human BBB model derived from hematopoietic stem cells as described by Cecchelli et al. (2014). Since the transporters involved in the transport of baclofen across the BBB in humans are unknown, it is assumed

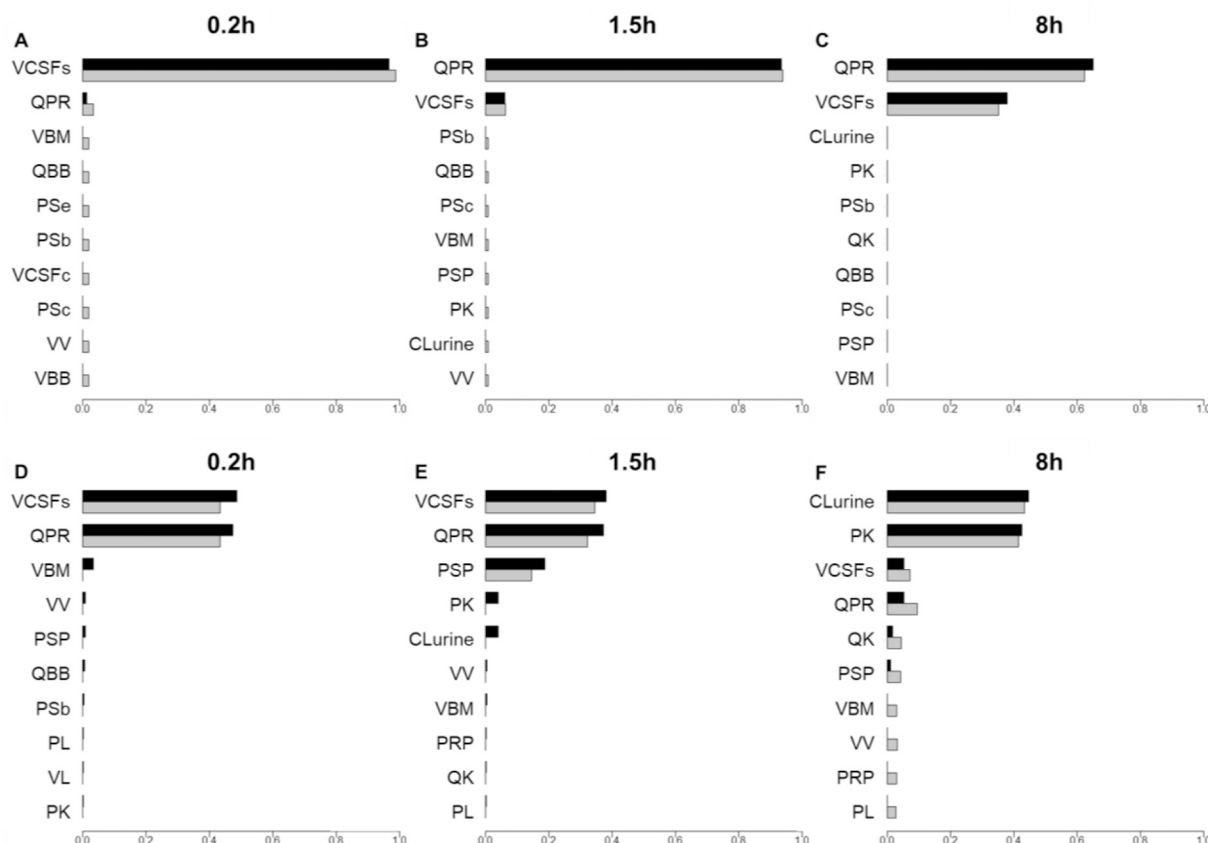


**Fig. 7.** Global sensitivity analysis of the baclofen adult population PBK model following intrathecal administration. The ten parameters having the largest influence on the spinal cord CSF concentration simulations (A–C) and the venous blood concentration simulations (D–F) are depicted at various timepoints, following a single intrathecal dose (0.1 mg). Black and grey depict the total and main sensitivity, respectively. 0.2 h: immediately following administration, 1.5 h: initial elimination phase in spinal cord CSF, overlapping with the  $T_{max}$  (time  $C_{max}$  is reached) of the venous blood concentration, 8 h: delayed elimination phase. QPR: Qproductionrate.

that this BBB model is representative of the *in vivo* situation and comprises both the in- and efflux transporters responsible for the transport of baclofen across the BBB.

**2.1.1.1. Chemicals and materials.** Baclofen (MW = 213.66 g/mol) and the fluorescent integrity marker Lucifer yellow (LY; MW = 457.25 g/mol) and dimethyl sulfoxide (DMSO), were purchased from Sigma-Aldrich (St. Quentin Fallavier, France). Acetonitrile, formic acid (FA), and ammonium formate were all high-performance liquid chromatography (HPLC) grade and were obtained from BioSolve (Valkenswaard, the Netherlands). HPLC grade water was obtained by a Milli-Q integral water purification system (Millipore Merck, Darmstadt, Germany).

#### 2.1.1.2. Human *in vitro* BBB model

**2.1.1.2.1. Hematopoietic stem cell-derived endothelial cells (ECs).** The human *in vitro* BBB model used in this study was modified from the co-culture model of Cecchelli et al. (Cecchelli et al., 2014). In brief, hematopoietic stem cell-derived ECs were isolated according to the method described in Cecchelli et al. (Cecchelli et al., 2014). Vials of frozen ECs ( $1 \times 10^6$  cells) were rapidly thawed and seeded in gelatin-coated (type A from porcine skin) (Sigma-Aldrich) 100-mm Petri dishes (Costar, Corning Incorporated, NY, USA) containing complete medium for ECs (endothelial cell medium (ECM) (Sigma-Aldrich), supplemented with 5% fetal calf serum (FCS) (Integro), 1% endothelial cell growth supplement (ECGS) (Sigma-Aldrich) and 0.5% gentamicin (Biochrom AG, Berlin, Germany)). Two days after thawing, around  $5 \times 10^6$  cells were present and ECs were trypsinised with trypsin/ ethylenediaminetetraacetic acid (EDTA) (0.05%/0.02% in phosphate

buffered saline – calcium and magnesium free (PBS-CMF) (Biochrom AG) and seeded on a semi-permeable Transwell insert (0.4  $\mu$ m, 12-well system, Costar, Corning Incorporated) coated with Matrigel (growth factor reduced BD Matrigel Matrix, BD Biosciences), at a concentration of  $16 \times 10^4$  cells per mL (or 80.000 cells per well). Cells were cultivated at 37 °C in a humidified atmosphere at 5%  $CO_2$ /95% air and medium was changed every two days. All sera were heat-inactivated before use.

**2.1.1.2.2. Co-culture of stem cell-derived endothelial cells (ECs) with brain pericytes.** Two days before ECs were put in co-culture, bovine brain pericytes were thawed. Primary bovine brain pericytes were isolated according to the method described by Vandenhoute et al. (Vandenhoute et al., 2011). Vials of frozen primary bovine brain pericytes (passage  $\leq 3$ ;  $1 \times 10^6$  cells) were rapidly thawed and seeded in gelatin-coated 100-mm Petri dishes containing complete medium for bovine pericytes (DMEM supplemented with 20% FCS, 1% L-glutamine and 0.5% gentamicin). After two days, pericytes were trypsinised and seeded, at a concentration of  $1.25 \times 10^4$  cells per  $cm^2$  (or 50.000 per well) on the bottom of gelatin-coated 12-well plates.

Co-cultures were initiated by inserting the Transwell inserts with attached ECs into the pericyte-containing well plates and by a subsequent change of the medium to ECM, resulting in a *non-contact* BBB *in vitro* model, as no physical interaction exist between the two cell types. Experiments were initiated after 6 days of co-culture. Co-cultures were cultivated at 37 °C in a humidified atmosphere and 5%  $CO_2$ . All sera were heat-inactivated before use.

**2.1.1.2.3. *In vitro* transport studies.** Transport studies were initiated after 6 days of co-culture for the human *in vitro* BBB model and all experiments were carried out at pH = 7.4 and  $T = 37$  °C.

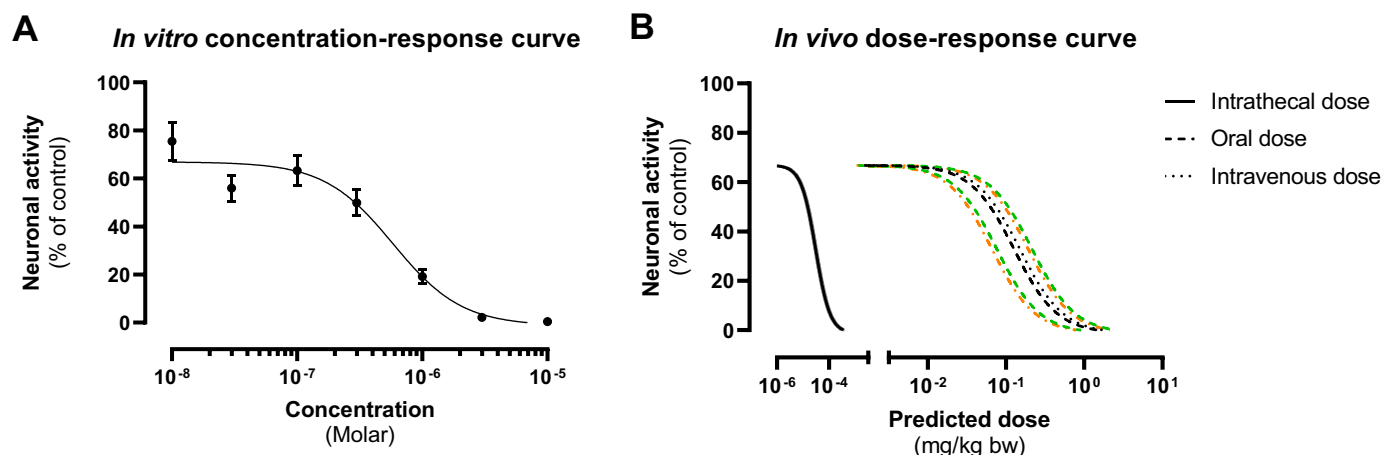


**Fig. 8.** *In vitro* concentration-response curve and *in vivo* dose-response curves for inhibition of neuronal activity by baclofen. (A): *In vitro* concentration response curve for the inhibition of neuronal activity by baclofen. Neuronal activity is depicted as the mean effect (compared to baseline activity) on spike rate  $\pm$  SEM for 23–26 wells on 4–5 plates. (B): Extrapolated median (black) *in vivo* dose-response curves for human exposure to baclofen including 5th and 95th percentile of the population (grey: intrathecal; green: oral; orange: intravenous). Dose-response curves for intrathecal, oral and intravenous administration (in  $\text{mg}\cdot\text{kg}^{-1}$  body weight) are estimated based on  $C_{\text{max}}$  values simulated using the adult population models. (For interpretation of the references to colour in this figure legend, the reader is referred to the web version of this article.)

Baclofen was first dissolved at a concentration of 5 mM in DMSO to obtain a stock solution. Then baclofen was dissolved at 5  $\mu\text{M}$  in Krebs-Ringer HEPES (RH) buffer (NaCl 150 mM, KCl 5.2 mM,  $\text{CaCl}_2$  2.2 mM,  $\text{MgCl}_2$  0.2 mM,  $\text{NaHCO}_3$  6 mM, glucose 2.8 mM, HEPES 5 mM, sterile water for injection – pH: 7.4) containing Lucifer yellow (LY) at 50  $\mu\text{M}$  and 0.1% human serum albumin (hSA, Sigma-Aldrich). 500  $\mu\text{L}$  was added to the luminal (donor) compartment of the BBB model whereas the abluminal (receiver) compartment was filled with 1.5 mL of RH. The plate was subsequently incubated at 37  $^{\circ}\text{C}$  on an orbital shaker (PX-MIS 6–1, Polymix, Kinematica AG, Switzerland) with low shaking velocity (60 rpm) for exactly 60 min.

After 60 min at 37  $^{\circ}\text{C}$ , an aliquot from each donor and receiver compartment was withdrawn and stored below  $-65$   $^{\circ}\text{C}$  until analysis. All experiments were performed at least in triplicate.

Apparent permeability coefficients ( $P_{\text{app}}$ ) for baclofen and LY were calculated according to the following equation:

$$P_{\text{app}} (\text{cm}\cdot\text{s}^{-1}) = \frac{J (\text{amount}\cdot\text{s}^{-1})}{S (\text{cm}^2)\cdot C_0 (\text{amount}\cdot\text{mL}^{-1})}$$

where  $J$  (in  $\text{amount}\cdot\text{s}^{-1}$ ) is the rate of appearance or flux of the compound in the receiver,  $S$  (in  $\text{cm}^2$ ) is the membrane surface area and  $C_0$  (in  $\text{amount}\cdot\text{mL}^{-1}$ ) is the initial donor concentration at  $t_0$ .

Possible compound loss was assessed by calculating the recovery (mass balance) according to the equation: Recovery (%) =  $(\text{CDF} + \text{CRfVR})/(\text{CD}_0\text{VD}) \times 100$ , where  $\text{CDF}$  = final concentration of the compound in the donor;  $\text{CRf}$  = final concentration of the compound in the receiver compartment;  $\text{CD}_0$  = initial concentration in the donor compartment;  $\text{VD,VR}$  = volumes in the donor and receiver compartments, respectively.

**2.1.1.2.4. Analytical procedures.** The amount of LY was determined

by fluorescence spectrophotometry (Synergy H1, BioTek Instruments SAS, Colmar, France) with an excitation wavelength of 432 and an emission wavelength of 538 nm. A blank value was subtracted from the measured values.

The quantification of baclofen was performed by Ultra-high performance liquid chromatography - tandem mass spectrometry (UHPLC-MS/MS).

Sample aliquots were subjected to protein precipitation with ice cold acetonitrile. After centrifugation for 20 min at 13200 rpm (MiniSpin plus, Vaudaux-Eppendorf), the supernatant were transferred into a 96-deep well plate, dried in nitrogen (Evaporex EVX-96, Apricot Designs, Monovia, CA, USA) and reconstituted with injection solvent (65% water containing 0.1% FA (i.e. mobile phase A) and 35% acetonitrile containing 0.05% FA (i.e. mobile phase B), v/v) before injection into the UHPLC-MS/MS (1290 Infinity UHPLC system coupled to a 6460 Triple quadrupole mass spectrometer, all Agilent, Waldbronn, Germany). The flow rates were set at 0.5 mL/min. Measurements were performed in electrospray ionization positive ion mode (ESI+) and multiple reaction monitoring mode. MS/MS parameters were as follows: drying gas (nitrogen) temperature and flow rate were 320  $^{\circ}\text{C}$  and 10 L/min, respectively, nebulizer pressure was 20 psi, sheath gas temperature was 400  $^{\circ}\text{C}$  and flow rate was 11 L/min. Nitrogen was used as collision gas. Data were acquired and quantifications were done using MassHunter (version B.08.02).

### 2.1.2. PBK models for baclofen in single adult

The models were constructed for an average man of 25 years, 175 cm and 70 kg and for an average woman of 25 years, 160 cm and 55 kg. The simulations were evaluated using clinical data from Kroin and Penn (1992; intrathecal), Sallerin-Caute et al. (1991; intrathecal), Kochak et al. (1985; oral), Schmitz et al. (2017; oral and intravenous) and

**Table 1**

$\text{IC}_{50}$  values (including 95% confidence intervals [CI]) corresponding to the *in vivo* dose-response curves depicted in Fig. 8B. The  $\text{IC}_{50}$  values for the median of the population and the 5th and 95th percentiles of the population (lower- and upper bounds) are depicted in  $\mu\text{g}$  for intrathecal administration and in mg for oral and intravenous administration. Doses are converted from mg/kg to mg by multiplying with the average body weight of the entire simulated population (75.5 kg).

Dosing	$\text{IC}_{50}$ Median [95% CI]	$\text{IC}_{50}$ 5th percentile [95% CI]	$\text{IC}_{50}$ 95th percentile [95% CI]
Intrathecal ( $\mu\text{g}$ )	2.3 [1.5–3.7]	2.1 [1.4–3.4]	2.5 [1.6–4.0]
Oral (mg)	9.6 [6.2–15]	5.8 [3.7–9.3]	16 [11–26]
Intravenous (mg)	11 [7.4–18]	5.0 [3.2–8.0]	15 [9.4–23]



Agarwal et al. (2015; oral and intravenous), with an age between 20 and 56 years and an unknown weight (see Methods Table S4 in Supplementary Information for more details on the evaluation data used in this study). The simulations from the single male and female adult models, as well as the male and female population models were compared to these studies.

### 2.1.3. PBK models for baclofen in single child

The PBK models for baclofen in a single child were based on an 11-year-old boy (140 cm and 36 kg) and a 9-year-old girl (120 cm and 26 kg; based on the evaluation study (Wiersma et al., 2003)). Chemical-specific and physiological parameters are listed in Methods Table S2 and Table S3 in the Supplementary Information. Physiological parameters were adjusted based on age, height and weight. Some assumptions were made for the paediatric models: [1] the absorption rate ( $k_a$ ) for children was set equal to the adult value (1.34; see Supplementary Methods Table S2), [2] permeability of the paediatric CNS barriers is solely dependent on brain volume (scaled to brain volume) and not the age-dependent activity of in- and efflux transporters, [3] CSF production rate is set to the adult production rate as the production rate is comparable in children of five years and older (Cutler et al., 1968).

### 2.1.4. PBK model for baclofen in adult and paediatric populations

The single adult and single paediatric models were converted to population models by incorporating variability for chemical-specific parameters and physiological parameters according to eq. 1:

$$P_i = P_{pop} * e^{Z\eta}$$

where  $P_i$  is the parameter for the specific individual,  $P_{pop}$  is the population average,  $Z$  is the standard normal variable and  $\eta$  is the variance (Verscheijden et al., 2019). Variances were derived from literature or set at 10% if no specific variance was known (see Methods Table S2 and Table S3 in Supplementary Information). As renal clearance is known to vary heavily, variance was put at 30% (Gowans and Fraser, 1988). For the absorption rate constant ( $k_a$ ), a truncated normal distribution was used to incorporate variability. Because all physiological parameters are dependent on age, body height, body weight and sex, an individual with a lower body weight would on average get a smaller organ volume, resulting in physiologically plausible individuals. The population PBK models were compared to the same evaluation studies as the single models, as described in Section 2.1.2. Studies with time-concentration profiles following a single dose were used to evaluate the PBK models developed in this study.

## 2.2. Global sensitivity analysis

The function 'soboljansen' was used in the R package 'sensitivity' to perform the global sensitivity analysis (Iooss et al., 2020). The impact of 50 parameters on model output was investigated according to the Sobol method (Iooss et al., 2020; Sobol et al., 2007). The global sensitivity analysis ranks the parameters according to their influence on the output, either venous blood concentration or spinal cord CSF concentrations. This identifies the main contributors to variability in the output at eight different timepoints after intrathecal, oral and intravenous administration: 0.2 h, 0.5 h, 1 h, 1.5 h, 2 h, 3 h, 4 h and 8 h. Uniform distributions were assigned to each parameter, with the minimum at 0.9 x median and the maximum at 1.1 x median. The complete R code for the sensitivity analysis can be found in the Supplementary Information ('Supplementary Models').

## 2.3. In vitro neurological effects of baclofen

Baclofen is a gamma-aminobutyric acid (GABA)-B receptor agonist used to treat spasticity (Simon et al., 2018). The stimulation of the GABA-B receptor by GABA or agonists reduces the frequency of action

potentials, which in turn reduces neurotransmitter release. As such, the GABA-B receptors are inhibitory receptors which, when stimulated, inhibit the continuation of neuronal signalling between neurons (Hondebrink et al., 2016). Neuronal activity, the signalling between neurons, can be measured *in vitro* using rat primary neuronal cultures grown on microelectrode arrays. Neuronal activity measurements were performed to determine the *in vitro* concentration-response curves of baclofen.

To obtain rat cortical cultures, animals were used in agreement with Dutch law, the European Community directives regulating animal research (2010/63/EU) and approved by the Ethical Committee for Animal Experiments of Utrecht University. In short, mixed males + females, neonatal Wistar rats, 0–1 postnatal, were prepared and cultured as discussed in Zwartsen et al. (2018). Next, neuronal activity of rat primary cortical cultures was measured prior to and following exposure to baclofen using the Maestro 768-channel amplifier (Axion BioSystems Inc., Atlanta, USA), as discussed in more detail in Zwartsen et al. (2018). The suppliers of the commercially used materials can also be found in Zwartsen et al. (2018). Neuronal cultures were exposed for 30 min to 0.01–10  $\mu\text{M}$  baclofen dissolved in and diluted using assay medium (Neural Basal-A supplemented with 25 g  $\text{L}^{-1}$  sucrose, 450  $\mu\text{M}$  L-glutamine, 1% penicillin/streptomycin, 2% mL B-27plus and 100 mM NaOH (for baclofen solubility)). Raw data files were rerecorded using the AxIS spike detector with specific thresholds previously described (Zwartsen et al., 2019). As baclofen showed transient effects, only the effects following the first 10 min of exposure were used and expressed as a percentage of baseline activity (for reference activity, inherent to different networks). The results on the mean spike rate from 24 to 26 wells on 4–5 plates were combined and outliers (effects 2 $\times$  standard deviation above or below average; 4.0%) were removed. Effects, averaged per concentration, were used for further statistical analyses. Non-linear regressions were used to graph the concentration-response curve and calculate inhibitory concentrations ( $\text{IC}_{50}$ ) (GraphPad Prism v8, La Jolla CA, USA).

## 2.4. Quantitative in vitro to in vivo extrapolation

Using the population PBK models and the *in vitro* neuronal activity concentration-response relationships, intrathecal, oral and intravenous doses leading to the inhibition of neuronal activity were predicted. For the extrapolation from *in vitro* to *in vivo* effects, it is assumed that only the free fraction of baclofen is able to induce effects. *In vitro* concentrations are directly related to CSF concentrations in the spinal cord (site of action) as no serum was used in the *in vitro* assay and baclofen is  $\sim 100\%$  unbound in CSF (Friden et al., 2009). Intrathecal, oral and intravenous doses were determined corresponding to  $C_{\text{max}}$  values in the spinal cord CSF compartment that correspond to a specific nominal *in vitro* concentration. In doing so, the *in vitro* concentration-response relationships were translated into predicted *in vivo* human bioequivalent dose-effect relationships for each administration route and compared to each other.

## 3. Results

### 3.1. BBB permeability

Baclofen was fully recovered from both sides of the BBB in the human *in vitro* BBB model, confirming the negligible loss of baclofen due to adsorption to the transwell plate, metabolism in the cells or insolubility. An *in vitro* apparent permeability ( $P_{\text{app}}$ ) value of  $1.57 \times 10^{-5} \text{ cm sec}^{-1}$  was determined (Culot, unpublished). This moderate  $P_{\text{app}}$  value was not influenced by the effect of baclofen on the BBB tightness, as the amount of lucifer yellow transferring over the BBB was comparable in both the absence ( $0.47 \times 10^{-5} \text{ cm sec}^{-1}$ ) and presence ( $0.55 \times 10^{-5} \text{ cm sec}^{-1}$ ) of baclofen. One limitation of  $P_{\text{app}}$  is that it does not account for the compound permeability across the cell-free filter. However, the  $P_{\text{app}}$  of lucifer yellow and baclofen across cell-free filter (respectively 2.47 and

$6.21 \times 10^{-5} \text{ cm sec}^{-1}$ ) demonstrate that the ability of the compounds to cross the insert is negligible in experiments with cells. The Papp value was used in the PBK model to derive the passive permeability surface area products for the BBB and the BCSFB (PSb and PSc, respectively).

### 3.2. Setup and evaluation of PBK models for single adult

As a starting point, a four compartment CNS-PBK model with intrathecal, oral and intravenous administration routes was coded and evaluated for a single male adult in both Berkeley Madonna and R.

Fig. 2A-C depict that the models in Berkeley Madonna and R simulate comparable spinal cord CSF and plasma concentrations, except after intravenous administration (all maximum concentrations and associated timepoints (C<sub>max</sub> and T<sub>max</sub>, respectively) and area under the curve (AUC) values can be found in Results Table S1 in the Supplementary Information). Following all administration routes, CSF concentrations in the spinal cord and plasma concentrations were slightly higher in the female model (C<sub>max</sub> ~1.2–1.4 fold higher, Results Fig. S1 and Results Table S1 in Supplementary Information), which is attributable to the lower tissue volumes and higher fat content in the female model. The male model was evaluated visually by comparing predicted and observed values of plasma- and CSF concentrations following intravenous and oral doses and following intrathecal doses, respectively. Simulations of the CSF concentration in the spinal cord following intrathecal administration are supported by clinical data from Kroin and Penn (1992) and Sallerin-Caute et al. (1991) (Fig. 2A). All simulations following intrathecal doses deviated on average 2.1-fold from the observed data, with some concentrations being overpredicted by the model. Plasma concentrations following oral and intravenous doses were supported by the data from Kochak et al. (1985) and Agarwal et al. (2015), respectively (Fig. 2B & C). All simulations following oral doses deviated on average 1.5-fold from the observed data. For intravenous administration, all simulations deviated on average 1.4-fold from the observed data.

### 3.3. Setup and evaluation of PBK models for single child

Next, single male and female paediatric models were developed. The model simulations were evaluated using measured plasma concentrations of the only paediatric study available in male and female patients (age 8–12 years) with gastroesophageal reflux disease (Wiersma et al., 2003). Data from the patients in this study supported the plasma concentrations of males well and all simulations deviated on average 1.3-fold from the observed data (Results Fig. S2 in Supplementary Information). Comparable to the adult model, differences in simulated tissue concentrations were indiscernible between the models in Berkeley Madonna and R (Results Table S1 in Supplementary Information). Like is the case with the adult models, spinal cord CSF and plasma concentrations were slightly higher in the female paediatric model following all administration routes (C<sub>max</sub> ~1.2–1.4-fold higher, Fig. 3 and Supplementary Information Table S1). When doses were adjusted for body weight, C<sub>max</sub> in paediatrics is lower than in adults (Results Fig. S3 in Supplementary Information).

### 3.4. Setup and evaluation of the adult and paediatric population models

Following the single models, both adult and paediatric population models were developed and evaluated for a population of 2000 individuals in total (1000 males and 1000 females) by varying most parameters (Methods Table S2 and Table S3 in Supplementary Information, Fig. 4 and Fig. 5). For these models, the same evaluation data were used as for the single models. Following intrathecal administration in the adult model, all, but three, clinical data points fell within the 95% confidence interval limits of the simulated population median (Fig. 4A). Following oral and intravenous administration, respectively 78% and 90% of all clinical data fell within the 95% confidence interval

limits of the simulated population median. For oral administration, some data were slightly overestimated by the model. The population models predict the C<sub>max</sub> accurately, but the models slightly underestimate the clearance of the chemical from CSF and plasma (Fig. 4). For the oral paediatric model, except two datapoints, all clinical data fell within the 95% confidence interval limits of the simulated population mean (Fig. 5E).

Using the population models, it was calculated that following all three administration routes, the C<sub>max</sub> of both the spinal cord CSF and the plasma concentrations were different between males and females and between adults and children, except for the plasma concentrations after intravenous administration between adults and children (see Results Tables S2 and S3 in Supplementary Information:  $p < 0.05$ ). When comparing the simulations from the adult population model with the simulations from the paediatric population model, the simulated maximum plasma and spinal cord CSF concentrations in the paediatric model were 1.5–2.2-fold lower than in the adult model, when the doses were adjusted for body weight (Results Table S3 in Supplementary Information). Simulated maximum concentrations of baclofen in the spinal cord CSF are ~4600 and ~4150 times lower at a dose of 0.1 mg following oral and intravenous administration, respectively, compared to intrathecal administration. Most data were within a two-fold change of the measured clinical evaluation data as can be seen in the observed vs. predicted plots (Fig. 6A–H). At low concentrations following intrathecal administration, a discrepancy between observed and predicted values is visible.

### 3.5. Sensitivity analysis

A global sensitivity analysis was performed to investigate the effect of the model input parameters on the simulation variance. The ten parameters influencing the simulations of the spinal cord CSF and venous blood concentrations following intrathecal administration most are depicted in Fig. 7 for three different timepoints. The results of the sensitivity analyses for all other timepoints and administration routes can be found in Results Fig. S4 in the Supplementary Information.

The global sensitivity analysis depicts that the volume of the spinal cord CSF (VCSFs) has the largest influence on the simulation of CSF concentrations in the spinal cord immediately following intrathecal administration (Fig. 7A). In the initial elimination phase (0.5–1 h), the production rate of the CSF (Q<sub>productionrate</sub>) becomes increasingly important and after 1.5–2 h, the Q<sub>productionrate</sub> is the only parameter with a large sensitivity. In the delayed elimination phase, the VCSFs becomes increasingly important again, although the Q<sub>productionrate</sub> remains to have the largest influence on the simulations (Fig. 7B–C). In venous blood, the same parameters have the largest influence at the first timepoints following intrathecal administration (0.2–2 h; Fig. 7D–E). However, from 3 h onwards, the distribution to the kidney (kidney partition coefficient PK) and the clearance (CL<sub>urine</sub>) become increasingly important and are the main contributing parameters at 8 h (Fig. 7F).

Following oral and intravenous administration, the VCSFs and the Q<sub>productionrate</sub> also greatly influence the CSF concentrations in the spinal cord at the earlier timepoints, although less strongly than after intrathecal administration (Results Fig. S4C and E in Supplementary Information). This gradually switches after 3–4 h to PK and CL<sub>urine</sub>. For oral administration specifically, the absorption rate constant (k<sub>a</sub>) has a large influence on plasma and spinal cord CSF concentrations (Results Fig. S4C and D in Supplementary Information). Other parameters that influence plasma concentrations most after oral and intravenous administration are PSP (partition coefficient slowly perfused tissue), PK and CL<sub>urine</sub> (Results Fig. S4D and F in Supplementary Information).

### 3.6. Quantitative in vitro to in vivo extrapolation

Using *in vitro* neuronal activity measurements performed on rat

primary cortical cultures grown on microelectrode arrays, the potency of baclofen to affect signal transduction was investigated. Baclofen concentration-dependently inhibited the neuronal activity with an  $IC_{50}$  value of  $0.59 \mu\text{M}$  [95% confidence interval:  $0.38\text{--}0.94$ ] (Fig. 8A). Complete inhibition of neuronal activity was seen at  $\geq 3 \mu\text{M}$ . The initial drop in neuronal activity following the lowest tested concentration is thought to be due to a (unknown) reaction between the solvent and the chemical since lowering the concentration did not reveal a biphasic effect (data not shown).

Using this concentration-response curve and the evaluated adult population-based PBK model for baclofen, an estimation of the equivalent intrathecal, oral and intravenous doses of baclofen affecting neuronal activity was made. As depicted in Fig. 8B, lower doses (in  $\text{mg}\cdot\text{kg}$  body weight) of intrathecally administered baclofen as opposed to orally or intravenously administered baclofen are needed to inhibit neuronal activity. A summary of all  $IC_{50}$  values (including 95% confidence intervals) are depicted for the median of the population and 5th and 95th percentile of the population (the lower and upper bounds) in Table 1.

#### 4. Discussion

This study provides a NG-PBK model for adults and children with a specialised CNS compartment for the spasmolytic agent baclofen that is suitable to simulate time-resolved tissue concentrations for three different administration routes. PBK models make it possible to accurately describe the distribution of baclofen in tissues in adults and paediatrics. This is of interest as doses and plasma concentrations of baclofen cannot be related to (effective) brain concentrations (Simon et al., 2018), and measuring CSF concentrations is too invasive for general practice. Since total brain concentrations (brain mass plus cranial CSF) of baclofen following administration were unavailable, the use of flow-limited models was not possible. Instead of fitting parameters in the permeability-limited brain compartment using pharmacokinetic data from animal tests, this model used *in vitro* kinetic measurements to describe the transfer of baclofen over the BBB and *in silico* models to calculate partition coefficients. This resulted in a NG-PBK model without any fitted parameters. Moreover, *in vitro* neuronal activity measurements were used in combination with the fully parameterised PBK models for QIVIVE and oral, intravenous and intrathecal doses affecting neuronal activity were derived. The results show that accurate concentration-time profiles can be simulated for baclofen using a NG-PBK model without the need for additional *in vivo* input. Moreover, the results indicate that 4150 and 4600 times higher doses are needed to reach the same CSF concentrations after intravenous and oral administration, respectively, compared to intrathecal administration.

Previously, a PK-pharmacodynamic model was published that modelled the concentrations of baclofen in the CSF in humans after intrathecal administration and related these concentrations to measurements of spasticity (Heetla et al., 2016). As the distance from the injection site influences the concentration of pharmaceuticals in the CSF greatly, the PK model in this study divided the intrathecal space into 57 compartments (Bernards, 2006). Although baclofen CSF concentrations were related to pharmacodynamic data, the model is not physiologically based and focusses solely on the CSF. Moreover, only twelve patients were included in the study and the PK data could not be validated. In the current study, the spinal cord CSF was modelled as one compartment. This is reasonable, because the evaluation dataset used for intrathecal administration here (Kroin and Penn (1992); Sallerin-Caute et al. (1991)) dosed and sampled at the same site (or close to the dosing site) in the spinal cord CSF. Nevertheless, if other (clinical) questions need to be answered, splitting the intrathecal space may be a useful addition to the model that can help in determining the ideal position of the catheter tip or the concentration gradient in the spinal cord and spinal cord CSF for specific treatments.

Incorporating the BBB in PBK models can improve estimations of

CNS concentrations, especially for compounds like baclofen that are tightly regulated by the BBB. This was confirmed by our *in vitro* BBB permeability study, which showed a moderate Papp value for baclofen (Papp  $1.57\cdot 10^{-5} \text{ cm/s}$ ). In comparison, the Papp values of two other compounds, atenolol (hydrophilic slowly permeable molecule) and codeine (more lipophilic, fast rate of transport) are  $1.09\cdot 10^{-5}$  and  $4.67\cdot 10^{-5} \text{ cm/s}$ , respectively, in the same BBB model (Culot, unpublished). This illustrates that the rate of transport of baclofen is indeed limited by the BBB. If no BBB is included in the PBK model, the model should either fit a permeability constant (if the brain compartment is considered permeability limited) or a QSAR should be used to predict a brain-blood partition coefficient (if the brain compartment is considered blood-flow limited). However, a QSAR as used for the other tissue-blood partition coefficients in the model does not take into account the specific characteristics of the BBB and the BCSFB, including transporters. Using the *in vitro* BBB permeability of baclofen and the surface area of the BBB and the BCSFB, the *in vivo* permeability of the BBB and BCSFB was estimated and incorporated in the model as PSB and PSC.

Overall, the model results showed that most simulations overlap with measured concentration-time profiles within a 2-fold margin, which is considered adequate for using PBK models in risk assessment (IPCS, 2010). As the therapeutic index of baclofen is unknown, but listed as narrow (Arbouw et al., 2014), a 2-fold margin was considered relevant for baclofen. The population simulations indicate that the majority of the clinical pharmacokinetic data fall within the 95% confidence intervals of our simulated population. Some concentrations were, however, either under- or overpredicted by the model and the model seems to underpredict the clearance of baclofen from the CSF and the plasma. This might partly be due to discrepancies in the data of the validation studies. The under- or overpredictions can also be due to the fact that the current study simulates the concentration-time profiles without fitting any parameters. As a consequence, the input parameters obtained from single studies can impact the simulations heavily. The sensitivity analysis suggests that parameters influencing the simulations most are the absorption constant ( $k_a$ ), clearance (CL<sub>urine</sub>), partition to the kidney (PK), partition to the slowly perfused tissue (PSP), volume of the spinal cord CSF (VCSFs) and the production rate of the CSF (QPR). Four of these ( $k_a$ , CL<sub>urine</sub>, PK and PSP) are chemical-specific parameters and are either based on a few input studies or on QSARs. Moreover, the VCSFs and the QPR are known to vary heavily between humans (Gaohua et al., 2016) and may therefore explain why simulations are under- or overpredicting concentrations.

While it is known that the development of children influences many physiological parameters (Schmitt et al., 2017), quantitative data like protein expression of BBB and BCSFB transporters is mostly unavailable (Verscheijden et al., 2019). The development and use of a PBK model makes it possible to adjust for example transporter activity and other processes involved in drug disposition to accurate pharmacokinetic parameterization in paediatric PBK models (Verscheijden et al., 2020). However, the limited availability of these quantitative data complicates the implementation of paediatric PBK models in drug development to improve safety and reduce off-label use (Committee on Drugs, 2014), even though the traditionally used simple body weight-based scaling also ignores these developmental processes and has many other limitations (Verscheijden et al., 2020). PBK models usually can predict better concentration-time profiles than simple allometric scaling procedures (Verscheijden et al., 2020). This model is the first to simulate concentrations of an intrathecally administered drug in the CSF compartments of children. However, the model is at the moment only applicable for children aged 5–11. This is due to differences in physiological parameters between age groups (like maturation of the kidney) and some of the assumptions made (like production of the CSF). Although outside the scope of this study, the model may be modified to simulate plasma and CSF concentrations for children of all ages following more research on age-appropriate (physiological) parameters (Verscheijden et al., 2019).

The CSF concentrations in the spinal cord and the corresponding



dose simulated in the adult model were correlated to the *in vitro* neuronal activity effects using QIVIVE. The inhibition of neuronal activity was measured in rat primary cortical cultures, which generates challenges in translating these data to the inhibition of neuronal activity in humans. However, while there are ethical concerns to the use of primary cultures and knowledge on human *in vitro* neuronal cultures is increasing (Tukker et al., 2018), no well-established human model is developed yet (Tukker et al., 2016). Research has showed that for toxins like tetradotoxin and drugs like amphetamine comparable sensitivity for human cultures and rat cultures were seen, but that rat cortical cultures were more sensitive to methoxetamine compared to the human model (Hondebrink et al., 2017; Kasteel and Westerink, 2017). It was suggested that this could be the result of the relatively immature phenotype of the used human model or differences in receptor expression or isoforms. Also, assuming a narrow therapeutic index of baclofen, especially when administered intrathecally (Arbouw et al., 2014), comparing inhibitory concentration (e.g.  $IC_{50}$ ) values or benchmark dose (limits) to clinical doses is complex. In addition, the extent of the *in vitro* inhibition of neuronal activity is not (yet) linked to *in vivo* (therapeutic or toxic) effects. An *in vitro* effect is not necessarily adverse/therapeutic *in vivo*, because compensatory mechanisms that are not present in an *in vitro* system can compensate the effect of the chemical *in vivo*.

When comparing the extrapolated human equivalent effective ( $IC_{50}$ ) doses from our QIVIVE study with the therapeutic doses used in practice, the model estimates the oral and intravenous doses well (oral: predicted dose 6–16 mg vs. dose regimen 15–80 mg (FDA, 2019); intravenous: predicted dose 5–15 mg vs. dose regimen 5–15 mg (Agarwal et al., 2015; Schmitz et al., 2017)). On the contrary, the extrapolated intrathecal dose (2.1–2.5  $\mu$ g) differs >20-fold from intrathecally administered baclofen for therapeutic effects (50–100  $\mu$ g (FDA, 2011; FDA, 2015)). This discrepancy can be caused by the uncertainty around using an  $IC_{50}$  value as an estimate for a therapeutic effect of baclofen. Full inhibition of neuronal activity occurs at an intrathecal dose of 39  $\mu$ g, which is close to the therapeutic range. Moreover, this discrepancy can be due to the distribution of baclofen over the spinal cord (Bernards, 2006). The rapid decrease in baclofen concentration as a function of the distance from the administration site in the spinal cord CSF was measured and simulated by Heetla et al. (2016), who showed that most drug was recovered within one cm from the administration site. The model presented in this manuscript is evaluated with sampling data close to the administration site, while average CSF concentrations of the complete spinal cord will be lower. The inclusion of an injection site compartment into the spinal CSF did not improve simulations (data not shown). This shows that for intrathecal administration, a more elaborate PBK model describing the spinal cord in more compartments may further improve extrapolation of doses.

To determine the robustness of the PBK model, the model was coded in both Berkeley Madonna and R. Outputs were highly comparable, as demonstrated before (Lin et al., 2017). The limited deviations seen in CSF concentrations in the spinal cord following intravenous administration can be explained by the different ways the numerical solvers handle initial concentrations in compartments. This comparison also illustrates the limitations of Berkeley Madonna (version 8.3.18) for PBK modelling (no global sensitivity analysis). Berkeley Madonna is a user-friendly and fast differential equations solver, while R is open access and versatile high-level programming platform used in various areas of research.

In conclusion, this study presents a PBK model of baclofen with a specialised CNS compartment that accurately simulates concentrations of this drug, for adults and children, in plasma and CSF using *in vitro* data to describe the BBB permeability and without any fitting of parameters. Using this model, concentrations in the brain mass and other organs/tissues can also be simulated. The model highlights that *in vitro* data can provide a rapid and cheap alternative to *in vivo* data, both kinetic data and hazard characterization/dynamic data, which can be used as input for the model. Moreover, adaptation of the population model to an

individual model, to fit a patient's characteristics (like age, weight, clearance rates, etcetera), will aid patient-centred medicine. Despite the uncertainty around some parameters like the CSF production rate and the absorption rate constant, an accurate simulation of concentrations in tissues can be made while using these *in vitro* data, without the need for fitting parameters. Also, the combination of using *in vitro* BBB permeability, *in vitro* effect concentrations and PBK modelling is a significant contribution to the 3Rs (reduction, refinement and replacement of animal testing) (Paini et al., 2019). Because none of the parameters were fitted, the model is generic and can be applied to other compounds as well. Moreover, the QIVIVE approach in this study is an efficient way of correlating *in vitro* effects to *in vivo* doses.

## Funding

This research was supported by a 3R Stimulus Fund from the Animal Welfare Body Utrecht, (The Netherlands) and the Faculty of Veterinary Medicine (Utrecht University, the Netherlands).

## Declaration of Competing Interest

The authors declare that they have no known competing financial interests or personal relationships that could have appeared to influence the work reported in this paper.

## Acknowledgements

We thank the members of the *in vitro* toxicology research group (Institute for Risk Assessment Sciences (IRAS), Utrecht University, the Netherlands) for their helpful discussions. We also thank L. Dehouck and M. Heymans (Univ. Artois, Blood-Brain Barrier laboratory (LBHE), France) for the preparation of the human *in vitro* BBB model and M. Oufir (Pharmazentrum, University of Basel, Switzerland) for the HPLC analysis of baclofen. We would also like to thank Laurens Verscheijden for his useful input for the PBK model.

## Appendix A. Supplementary data

Supplementary data to this article can be found online at <https://doi.org/10.1016/j.tiv.2021.105223>.

## References

- Agarwal, S.K., Kriel, R.L., Cloyd, J.C., Coles, L.D., Scherckenbach, L.A., Tobin, M.H., et al., 2015. A pilot study assessing pharmacokinetics and tolerability of oral and intravenous baclofen in healthy adult volunteers. *J. Child Neurol.* 30 (1), 37–41.
- Arbouw, M.E., Hoge, H.L., Meulenbelt, J., Jansman, F.G., 2014. Increase of baclofen intoxications: risks involved and management. *Neth. J. Med.* 72 (9), 497–499.
- Bernards, C.M., 2006. Cerebrospinal fluid and spinal cord distribution of baclofen and bupivacaine during slow intrathecal infusion in pigs. *Anesthesiology* 105 (1), 169–178.
- Cecchelli, R., Aday, S., Sevin, E., Almeida, C., Culot, M., Dehouck, L., et al., 2014. A stable and reproducible human blood-brain barrier model derived from hematopoietic stem cells. *PLoS One* 9 (6), e99733.
- Committee on Drugs, 2014. Off-label use of drugs in children. *Pediatrics* 133 (3), 563–567.
- Cutler, R.W.P., Page, L., Galicich, J., Watters, G.V., 1968. Formation and absorption of cerebrospinal fluid in man. *Brain* 91 (4), 707–720.
- Dauer, W., Przedborski, S., 2003. Parkinson's disease: mechanisms and models. *Neuron* 39 (6), 889–909.
- de Lange, E.C.M., 2015. PBPK modeling approach for predictions of human CNS drug brain distribution. In: *Blood-Brain Barrier in Drug Discovery*. John Wiley & Sons, Inc., pp. 296–323.
- Deguchi, Y., Inabe, K., Tomiyasu, K., Nozawa, K., Yamada, S., Kimura, R., 1995. Study on brain interstitial fluid distribution and blood-brain barrier transport of baclofen in rats by microdialysis. *Pharm. Res.* 12 (12), 1838–1844.
- Drugbank, 2005. Baclofen. [Go.drugbank.com/drugs/DB00181](http://go.drugbank.com/drugs/DB00181).
- Fairman, K., Li, M., Kabadi, S.V., Lumen, A., 2020. Physiologically based pharmacokinetic modeling: a promising tool for translational research and regulatory toxicology. *Curr. Opin. Toxicol.* 23–24, 17–22.
- FDA, 2011. Lioresal Intrathecal: Baclofen Injection. Food & Drug Administration. [https://www.accessdata.fda.gov/drugsatfda\\_docs/label/2011/020075s021lbl.pdf](https://www.accessdata.fda.gov/drugsatfda_docs/label/2011/020075s021lbl.pdf).

- FDA, 2015. Gablofen (Baclofen Injection): Highlights of Prescribing Information. Food & Drug Administration. [https://www.accessdata.fda.gov/drugsatfda\\_docs/label/2015/022462s0081bl.pdf](https://www.accessdata.fda.gov/drugsatfda_docs/label/2015/022462s0081bl.pdf).
- FDA, 2019. OZOBAX (Baclofen) Oral Solution: highlights of Prescribing Information. Food & Drug Administration. [https://www.accessdata.fda.gov/drugsatfda\\_docs/label/2019/208193s0001bl.pdf](https://www.accessdata.fda.gov/drugsatfda_docs/label/2019/208193s0001bl.pdf).
- Fidler, M.L., Hallow, M., Wilkins, J., Wang, W., 2020. RxODE: Facilities for Simulating From ODE-Based Models. <https://CRAN.R-project.org/package=RxODE>.
- Friden, M., Winiwarter, S., Jerndal, G., Bengtsson, O., Wan, H., Bredberg, U., et al., 2009. Structure-brain exposure relationships in rat and human using a novel data set of unbound drug concentrations in brain interstitial and cerebrospinal fluids. *J. Med. Chem.* 52 (20), 6233–6243.
- Gaohua, L., Neuhoff, S., Johnson, T.N., Rostami-Hodjegan, A., Jamei, M., 2016. Development of a permeability-limited model of the human brain and cerebrospinal fluid (CSF) to integrate known physiological and biological knowledge: estimating time varying CSF drug concentrations and their variability using in vitro data. *Drug Metabol. Pharm.* 31 (3), 224–233.
- Gowans, E.M., Fraser, C.G., 1988. Biological variation of serum and urine creatinine and creatinine clearance: ramifications for interpretation of results and patient care. *Ann. Clin. Biochem.* 25 (Pt 3), 259–263.
- Heetla, H.W., Proost, J.H., Molmans, B.H., Staal, M.J., van Laar, T., 2016. A pharmacokinetic-pharmacodynamic model for intrathecal baclofen in patients with severe spasticity. *Br. J. Clin. Pharmacol.* 81 (1), 101–112.
- Hondebrink, L., Verboven, A.H.A., Drega, W.S., Schmeink, S., de Groot, M.W.G.D.M., van Kleef, R.G.D.M., et al., 2016. Neurotoxicity screening of (illicit) drugs using novel methods for analysis of microelectrode array (MEA) recordings. *NeuroToxicology* 55, 1–9.
- Hondebrink, L., Kasteel, E.E.J., Tukker, A.M., Wijnolts, F.M.J., Verboven, A.H.A., Westerink, R.H.S., 2017. Neuropharmacological characterization of the new psychoactive substance methoxetamine. *Neuropharmacology* 123, 1–9.
- Hoshi, Y., Uchida, Y., Tachikawa, M., Inoue, T., Ohtsuki, S., Terasaki, T., 2013. Quantitative Atlas of blood-brain barrier transporters, receptors, and tight junction proteins in rats and common Marmoset. *J. Pharm. Sci.* 102 (9), 3343–3355.
- Iooss, B., Da Veiga, Sebastien, Janon, Alexandre, Pujol, Gilles, Broto, Baptiste, Boumhaout, Khalid, et al., 2020. Sensitivity: Global Sensitivity Analysis of Model Outputs. <https://CRAN.R-project.org/package=sensitivity>.
- IPCS, 2010. Characterization and application of physiologically based pharmacokinetic models in risk assessment. World Health Organization, Geneva. Harmonization Project Document No. 9. [https://www.who.int/ipcs/methods/harmonization/areas/pbpb\\_models.pdf?ua=1](https://www.who.int/ipcs/methods/harmonization/areas/pbpb_models.pdf?ua=1).
- Kasteel, E.E.J., Westerink, R.H.S., 2017. Comparison of the acute inhibitory effects of Tetrodotoxin (TTX) in rat and human neuronal networks for risk assessment purposes. *Toxicol. Lett.* 270, 12–16.
- Kochak, G.M., Rakhit, A., Wagner, W.E., Honc, F., Waldes, L., Kershaw, R.A., 1985. The pharmacokinetics of baclofen derived from intestinal infusion. *Clin. Pharmacol. Ther.* 38 (3), 251–257.
- Kroin, J.S., Penn, R.D., 1992. Cerebrospinal fluid pharmacokinetics of lumbar intrathecal baclofen. In: Lakke, J.P.W.F., D., E., AWF, Rutgers (Eds.), Parenteral Drug Therapy in Spasticity and Parkinson's Disease. Parthenon Publishing, Carnforth (UK), pp. 67–78.
- Lin, Z., Jaber-Douraki, M., He, C., Jin, S., Yang, R.S.H., Fisher, J.W., et al., 2017. Performance assessment and translation of physiologically based pharmacokinetic models from acsX to Berkeley madonna, MATLAB, and R language: oxytetracycline and gold nanoparticles as case examples. *Toxicol. Sci.* 158 (1), 23–35.
- Loizou, G., Spendiff, M., Barton, H.A., Bessems, J., Bois, F.Y., d'Yvoire, M.B., et al., 2008. Development of good modelling practice for physiologically based pharmacokinetic models for use in risk assessment: the first steps. *Regul. Toxicol. Pharmacol.* 50 (3), 400–411.
- Mersmann, O., Trautmann, H., Steuer, D., Bornkamp, B., 2018. truncnorm: Truncated Normal Distribution. <https://CRAN.R-project.org/package=truncnorm>.
- Meythaler, J.M., Clayton, W., Davis, L.K., Guin-Renfroe, S., Brunner, R.C., 2004. Orally delivered baclofen to control spastic hypertonia in acquired brain injury. *J. Head Trauma Rehabil.* 19 (2), 101–108.
- Morris, M.E., Rodriguez-Cruz, V., Felmlee, M.A., 2017. SLC and ABC transporters: expression, localization, and species differences at the blood-brain and the blood-cerebrospinal fluid barriers. *AAPS J.* 19 (5), 1317–1331.
- Nestler, E.J., Barrot, M., DiLeone, R.J., Eisch, A.J., Gold, S.J., Monteggia, L.M., 2002. Neurobiology of depression. *Neuron* 34 (1), 13–25.
- Paini, A., Leonard, J.A., Joossens, E., Bessems, J.G.M., Desalegn, A., Dorne, J.L., et al., 2019. Next generation physiologically based kinetic (NG-PBK) models in support of regulatory decision making. *Comput. Toxicol.* 9, 61–72.
- Perry, C., Davis, G., Conner, T.M., Zhang, T., 2020. Utilization of physiologically based pharmacokinetic modeling in clinical pharmacology and therapeutics: an overview. *Curr. Pharmacol. Rep.* 1–14.
- Punt, A., Aartse, A., Bovee, T.F.H., Gerssen, A., van Leeuwen, S.P.J., Hoogenboom, R., et al., 2019. Quantitative in vitro-to-in vivo extrapolation (QIVIVE) of estrogenic and anti-androgenic potencies of BPA and BADGE analogues. *Arch. Toxicol.* 93 (7), 1941–1953.
- R Development Core Team, R: A Language and Environment for Statistical Computing. <https://www.R-project.org/>. R Foundation for Statistical Computing, Vienna, Austria.
- Rodgers, T., Rowland, M., 2006. Physiologically based pharmacokinetic modelling 2: predicting the tissue distribution of acids, very weak bases, neutrals and zwitterions. *J. Pharm. Sci.* 95 (6), 1238–1257.
- Rodgers, T., Leahy, D., Rowland, M., 2005. Physiologically based pharmacokinetic modeling 1: predicting the tissue distribution of moderate-to-strong bases. *J. Pharm. Sci.* 94 (6), 1259–1276.
- Sallerin-Caute, B., Lazorthes, Y., Monsarrat, B., Cros, J., Bastide, R., 1991. CSF baclofen levels after intrathecal administration in severe spasticity. *Eur. J. Clin. Pharmacol.* 40 (4), 363–365.
- Schmitt, G., Parrott, N., Prinssen, E., Barrow, P., 2017. The great barrier belief: the blood-brain barrier and considerations for juvenile toxicity studies. *Reprod. Toxicol.* 72, 129–135.
- Schmitz, N.S., Krach, L.E., Coles, L.D., Mishra, U., Agarwal, S.K., Cloyd, J.C., et al., 2017. A randomized dose escalation study of intravenous baclofen in healthy volunteers: clinical tolerance and pharmacokinetics. *PM&R* 9 (8), 743–750.
- Sharma, R.P., Schuhmacher, M., Kumar, V., 2018. Development of a human physiologically based pharmacokinetic (PBPK) model for phthalate (DEHP) and its metabolites: a bottom up modeling approach. *Toxicol. Lett.* 296, 152–162.
- Simon, N., Franchitto, N., Rolland, B., 2018. Pharmacokinetic studies of baclofen are not sufficient to establish an optimized dosage for management of alcohol disorder. *Front Psychiatry* 9, 485.
- Sobol, I.M., Tarantola, S., Gatelli, D., Kucherenko, S.S., Mauntz, W., 2007. Estimating the approximation error when fixing unessential factors in global sensitivity analysis. *Reliab. Eng. Syst. Saf.* 92 (7), 957–960.
- Stolp, H., Liddelow, S., Sá-Pereira, I., Dziegielewska, K., Saunders, N., 2013. Immune responses at brain barriers and implications for brain development and neurological function in later life. *Front. Integr. Neurosci.* 7 (61).
- Tukker, A.M., de Groot, M.W., Wijnolts, F.M., Kasteel, E.E., Hondebrink, L., Westerink, R.H., 2016. Is the time right for in vitro neurotoxicity testing using human iPSC-derived neurons? *ALTEX* 33 (3), 261–271.
- Tukker, A.M., Wijnolts, F.M.J., de Groot, A., Westerink, R.H.S., 2018. Human iPSC-derived neuronal models for in vitro neurotoxicity assessment. *NeuroToxicology* 67, 215–225.
- Vandenhoute, E., Dehouck, L., Boucay, M.C., Sevin, E., Uzbekov, R., Tardivel, M., et al., 2011. Modelling the neurovascular unit and the blood-brain barrier with the unique function of pericytes. *Curr. Neurovasc. Res.* 8 (4), 258–269.
- Verscheijden, L.F.M., Koenderink, J.B., de Wildt, S.N., Russel, F.G.M., 2019. Development of a physiologically-based pharmacokinetic pediatric brain model for prediction of cerebrospinal fluid drug concentrations and the influence of meningitis. *PLoS Comput. Biol.* 15 (6), e1007117.
- Verscheijden, L.F.M., Koenderink, J.B., Johnson, T.N., de Wildt, S.N., Russel, F.G.M., 2020. Physiologically-based pharmacokinetic models for children: Starting to reach maturation? *Pharmacol. Ther.* 107541.
- Weißhaar, G.F., Hoemberg, M., Bender, K., Bangen, U., Herkenrath, P., Eifinger, F., et al., 2012. Baclofen intoxication: a “fun drug” causing deep coma and nonconvulsive status epilepticus—a case report and review of the literature. *Eur. J. Pediatr.* 171 (10), 1541–1547.
- Wickham, H., ggplot2: Elegant Graphics for Data Analysis. <https://ggplot2.tidyverse.org>. Springer-Verlag, New York.
- Wiersma, H.E., van Bostel, C.J., Butter, J.J., van Aalderen, W.M., Omari, T., Benninga, M.A., 2003. Pharmacokinetics of a single oral dose of baclofen in pediatric patients with gastroesophageal reflux disease. *Ther. Drug Monit.* 25 (1), 93–98.
- Yamamoto, Y., Valitalo, P.A., Wong, Y.C., Huntjens, D.R., Proost, J.H., Vermeulen, A., et al., 2018. Prediction of human CNS pharmacokinetics using a physiologically-based pharmacokinetic modeling approach. *Eur. J. Pharm. Sci.* 112, 168–179.
- Zwartsen, A., Hondebrink, L., Westerink, R.H.S., 2018. Neurotoxicity screening of new psychoactive substances (NPS): effects on neuronal activity in rat cortical cultures using microelectrode arrays (MEA). *NeuroToxicology* 66, 87–97.
- Zwartsen, A., Hondebrink, L., Westerink, R.H.S., 2019. Changes in neuronal activity in rat primary cortical cultures induced by illicit drugs and new psychoactive substances (NPS) following prolonged exposure and washout to mimic human exposure scenarios. *NeuroToxicology* 74, 28–39.